Normal Stresses at the Tire-Soil Interface In Yielding Soils

D. R. FREITAG, A. J. GREEN and N. R. MURPHY, JR.
Respectively, Chief, Engineer, and Mathematician, Mobility Section, Mobility and Environmental Division, U. S. Army Engineer Waterways Experiment Station, CE, Vicksburg, Miss.

Small diaphragm-type pressure-sensitive cells were set flush with the outer surface of a smooth pneumatic tire. Tests were run to determine the magnitude and distribution of normal pressures at the tire-soil interface of a driven and a towed tire at several loads and inflation pressures.

Tests were conducted on both cohesive and noncohesive soils. The test soils were carefully prepared to a consistency that would allow the soil to yield under the applied load. In the tests reported, the different combinations of test variables produced ruts that ranged from a fraction of an inch to several inches in depth. Tire deflection measurements were made to determine the shape of the deformed tire and thereby to locate the position of the cells.

It was found that the pressure-distribution patterns that occur in the two soil types are different. Typical patterns are shown and some general relations between the patterns observed and the test variables are presented.

•THE U. S. Army Engineer Waterways Experiment Station at Vicksburg, Miss., is conducting systematic studies that will provide information on factors which influence vehicle mobility in deformable soils. The ultimate purpose of these studies is to develop rational means of designing military vehicles that will provide specified levels of performance in off-road conditions.

A study of the stresses at the interface of a moving pneumatic tire and the medium upon which it travels is one such study. Freitag and Green (1) gave results of a pilot study (conducted in the fall of 1961) to determine the distribution of stresses under pneumatic tires on an unyielding surface. Following this study, an extensive program was initiated to investigate and evaluate the factors that influence magnitude and distribution of the normal stresses between a pneumatic tire and deformable soils. While the objective of these studies is primarily military, the results will be applicable in many other fields. For instance, the development of knowledge pertaining to the stresses and strains or deformation at the tire-soil interface is important to the agricultural researcher who tries to minimize the compaction effect of pneumatic tires, and to the construction engineer who in many instances must depend on the kneading action of pneumatic tires to help compact a fill or subgrade material.

This paper describes the results of tests made to measure the distribution of stresses at the tire-soil interface under some representative test conditions. Two soils, a sand and a clay, carefully placed in a test pit, were used in the program. Each soil was tested at three different levels of strength. Only one tire at one test load was employed, but stresses were measured at several different inflation pressures. Tests were conducted with the wheel powered and with it towed.

Paper sponsored by Committee on Stress Distribution in Earth Masses.

TEST SOILS

Description

The sand used was a medium-to-fine sand, subangular in shape, poorly graded, and classified as SP according to the Unified Soil Classification System (USCS). The clay, taken from an alluvial deposit in the Vicksburg, Miss., area was classified as CH under the USCS. The gradation and classification data for both soils are shown in Figure 1.

Preparation

Sand. —The sand was placed in an open pit that had been lined with a waterproof membrane. This pit was approximately 4½ ft wide, 100 ft long, and 3½ ft deep.

After the pit was filled and subsequently after each test, the sand was loosened by tilling and then recompacted in place before the next test. Tilling was done with a simple multitooth scarifier that was pulled back and forth through the section until the sand was adequately loosened. The maximum depth of tillage possible with this equipment was 36 in. The actual depth of tillage and the amount of compaction necessary varied, depending on the soil strength desired and on the strength that had resulted from previous traffic on the section. The equipment used for tilling and compacting (scarifier and vibrator) was attached to the test carriage (described later) and towed at a uniform rate of speed (about 1.0 fps). The goal of the soil processing work was to obtain a test section in which the strength increased uniformly with depth and was consistent along the length of the test lane.

Cone index measurements were made to evaluate the effectiveness of the processing for each test. Cone index, an index of soil strength, is the force per unit area required to push a 30-deg right circular cone into the soil at a rate of 72 in. per min (2).

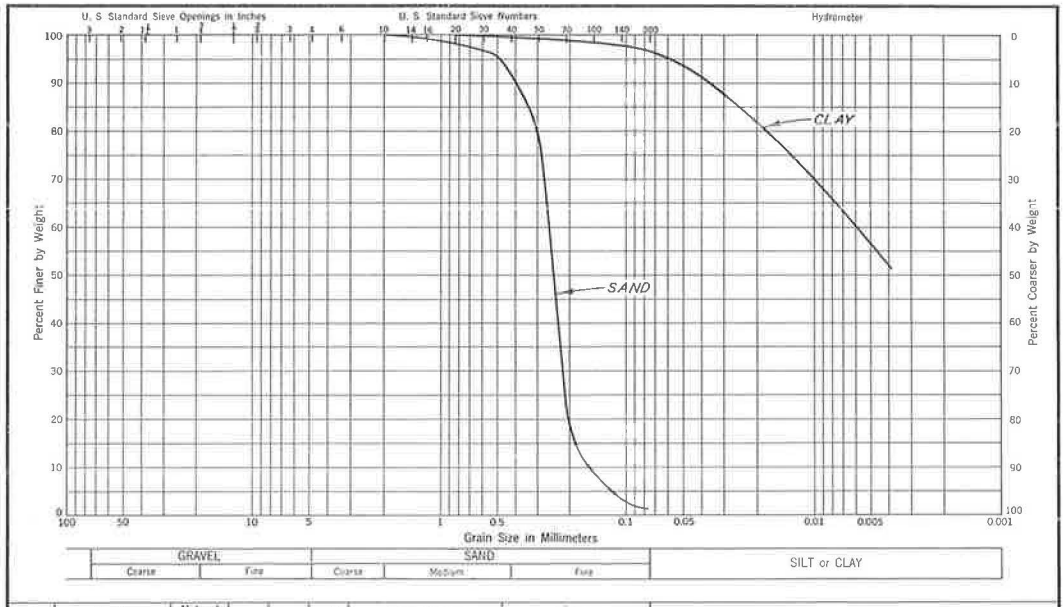

Number	Depth	Natural Moisture	L. L.	P. L.	P. I.	Classification	Density
						FINE SAND (SP)	MAX 106.1 LB/CU FT
							MIN 87.4 LB/CU FT
			64	22	42	HEAVY CLAY (CH)	

Figure 1. Gradation and classification data.

Clay. —A stockpile of natural clay was turned and worked until it had been air-dried to about 8 percent moisture content. The clay was then fed through a conveyor system that metered the soil into the hopper of a disintegrator. Here the lumps of soil were broken into smaller sizes and dropped into a roller crusher. The crusher broke the clods down to a maximum diameter of $\frac{1}{8}$ in. and fed them into a pug mill. A preselected quantity of water was metered into the pug mill and blended into the soil to provide uniform texture and the desired water content. The prepared soil issued continuously from the end of the pug mill and dropped into a truck. It was then transported to the test pit. The soil was dumped into the test pit in sufficient quantity to produce layers approximately 6 in. thick. Each layer was tilled with a pulvimixer and compacted by a pneumatic-tired roller. The compacted 6-in. layer was scarified to a depth of approximately $1\frac{1}{2}$ in. before the next soil layer was placed. The surface of each layer was moistened during construction to compensate for the loss in moisture due to evaporation. This procedure was continued until the top of the section was 1 to 2 in. above the desired grade. The excess material was then sliced off by a section of grader blade mounted on the test carriage, and the soil was allowed to "cure" for one or more days to insure a uniform moisture content throughout the section. In this case the goals of the soil processing were to obtain a strength profile that showed little or no increase in strength with depth, and to achieve a degree of saturation of 95 percent or greater in order to minimize the effects of traffic on soil strength.

Cone index measurements and moisture-density determinations were made to determine the effectiveness of the processing procedures. When a group of tests was conducted at a single soil strength, the fine-grained soil was reprocessed in place. This was done by backfilling the rut left by previous traffic, compacting the surface with pneumatic-tired and smooth-drum rollers, and then leveling the section. It was found that by sprinkling the surface of the section frequently and keeping it covered between actual test runs, the original strength of the material could be maintained for periods up to 60 days.

TEST APPARATUS

Test Carriage

Tests were conducted with a single-wheel test carriage that can accommodate wheels up to 56 in. in diameter and 26 in. in width. The carriage controls the path and alignment of the test wheel and is designed to isolate and measure the resultant horizontal and vertical forces and the torque at the wheel. Devices for determining degrees of tire rotation, forward travel of the carriage, and vertical movement of the hub of the test wheel are part of the system. Figure 2 is an overall view of this test carriage.

Instrumented Tire

Tire. —An 11.00-20, 12-ply rating, military tire from which all tread had been removed by buffing was used in this program. In buffing the tire, only the thickness of the lugs was removed so that the thickness and shape of the tire carcass were very nearly those of the original. Deflection gages were mounted inside the tire to determine changes in cross-sectional shape in the tire contact area. Stress cells, mounted in the tire so that their diaphragms were flush with the tire's outer surface, were used to measure normal stresses at the tire-soil interface during the operation.

Stress Cells. —Sever stress cells, 0.75 in. in diameter and 0.25 in. in height, were mounted in the face of the tire. On the basis of the type of construction (deflecting diaphragm) and the calibration procedures used, these cells are considered to measure stresses normal to their diaphragms. A protective steel cup around the cell prevents the tire from exerting pressure on the cell's sidewall, as such a pressure would cause the diaphragm to deflect and thus invalidate the pressure cell measurements. The walls and bottom of the cup are $\frac{1}{16}$ in. thick, and the inside radius of the cup is $\frac{1}{32}$ in. larger than that of the cell. A semiconductor strain gage constitutes the pressure-sensitive element of each cell, and resistors are used to complete a full Wheatstone bridge circuit. Figure 3 illustrates graphically the electrical circuit from the pressure cell to

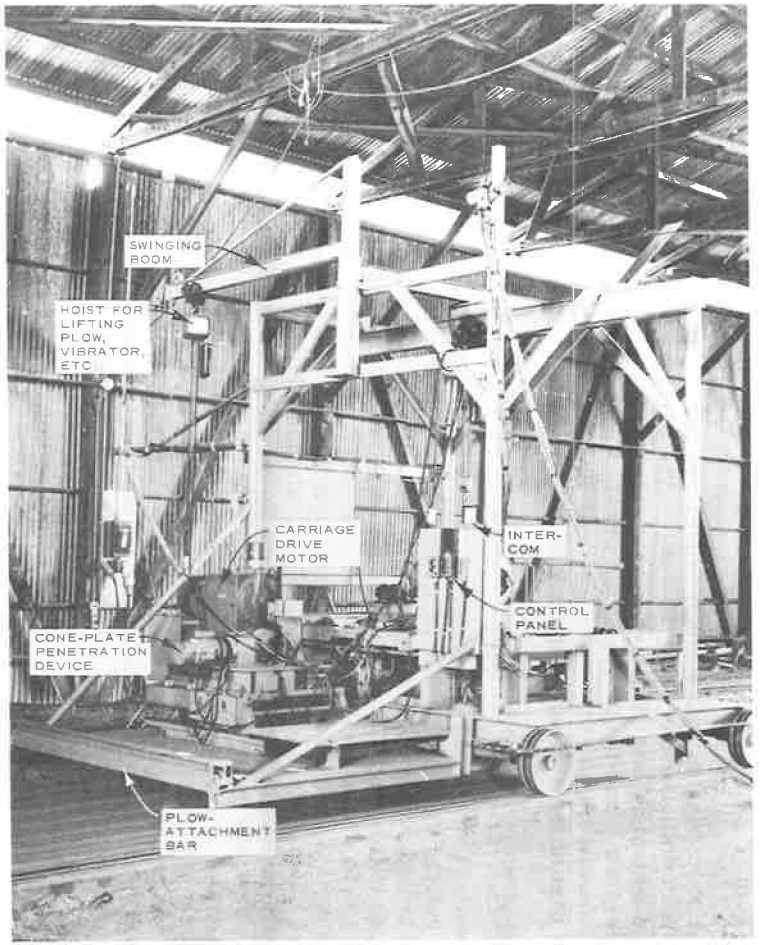

Figure 2. Rear view of large test rig.

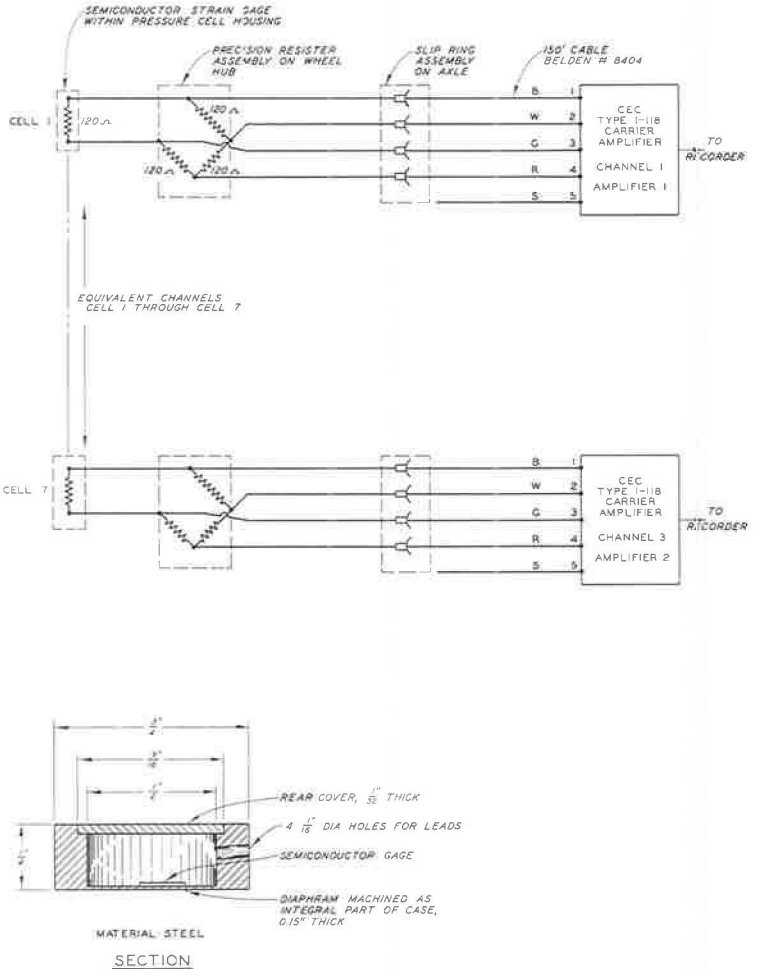

Figure 3. Electrical schematic drawing of WES pressure cell amplifier.

the recorder. The use of semiconductors permits the construction of a more durable gage, becuase they are much more sensitive than ordinary foil strain gages.

Seven holes, each large enough to accommodate a cell and cup as described in the preceding paragraph, were cut in the outer surface of the tire, and slits were cut leading from the holes to accommodate the conductor wires of each cell. The seven cells were installed along a diagonal line across the face of the tire (Fig. 4) to avoid serious weakening of the tire in the single cross-sectional plane. The total depth of the cell and cup was approximately equal to the thickness of the rubber over the outermost layer of cord, and for this reason extreme care had to be taken when cutting the tire to avoid damage to the cords. The bottom of the cup was bonded to the tire with a latex-adhesive. The area between the outer walls of the cup and the tire was backfilled with a pliable rubber-base compound that did not adhere to the tire or the cup. The cell was fastened to the cup with a thin layer of bituminous

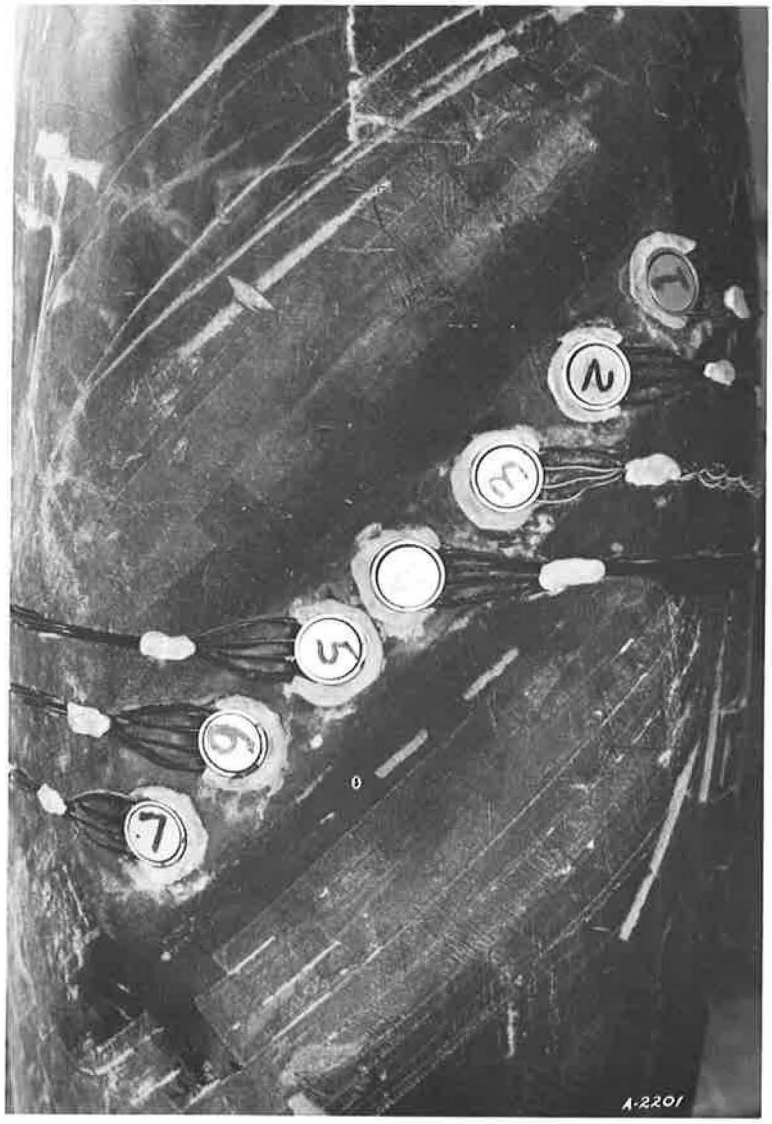

Figure 4. Cells in the tire carcass.

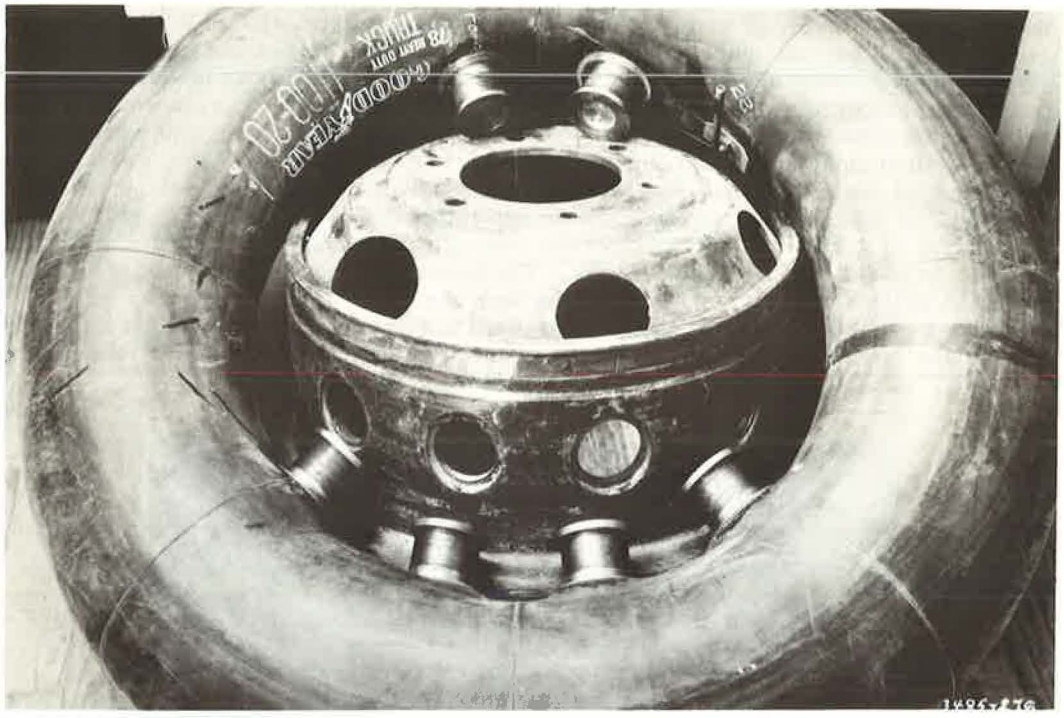

Figure 5. Deflection gage ports in 11.00-20 tube.

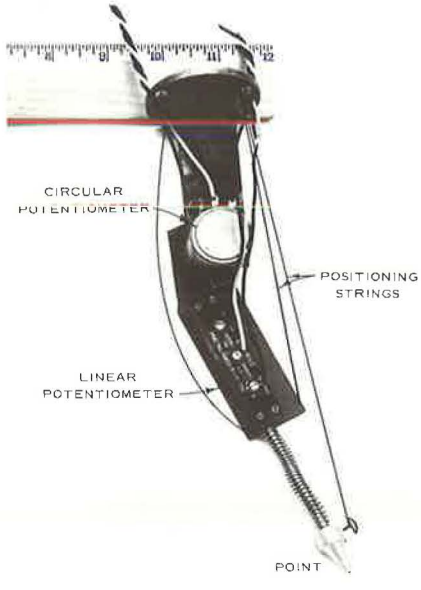

Figure 6. Deflection gage.

adhesive so that the cell would stay in place during traffic, but could be easily removed for calibration or repair. A strip of thin rubber membrane was used to cover the entire cell area to prevent damage to the diaphragm of the cell and to prevent sand from getting in the area between the cup and the wall of the cell. The membrane was fastened to the tire with a thin plastic adhesive tape that could deform as the tire carcass did without providing additional strength to the tire carcass.

Deflection Gages. —Commercially available linear and circular potentiometers were used to measure deflections inside the tire. A linear and a circular potentiometer were combined to make one gage and inserted through a port in the rim and tube (Fig. 5). A pointed brass tip attached to the end of the potentiometer shaft was held firmly against a point inside the tire by a spring. Movements of this point in line with the potentiometer shaft and in an arc around the center of rotation of the circular potentiometer were recorded. Five gages were employed, each positioned to record movements at a different point on the left-hand side of the tire. Because it was not physically possible to place more than one gage in the same cross-

section, they were placed in separate cross-sections normal to the plane of rotation of the tire. The gages were rotated to the desired angular position while outside the tire, and the circuit that included the circular potentiometer was balanced at that position. The gage was then placed in the port, and the base was tightened in position. After this had been done, the positioning strings (Fig. 6) were used to rotate the gage until the circular potentiometer circuit for that gage was rebalanced, indicating that the gage was in the desired position.

TEST CONDITIONS

Both towed- and powered-wheel tests have been conducted in sand, but to date only towed tests have been conducted in clay. Various combinations of load, inflation pressure, and soil strength were studied in the towed tests; during the powered-wheel tests, slip also was a controlled variable.

METHODS USED IN ANALYSIS OF TEST RESULTS

Data Reduction

In the form in which they are first obtained, the data are merely simultaneous records of the measurements. At each instant of time, data are recorded that describe the angular position of a stress cell relative to the wheel axle, the position of the cell or the deflected tire, the vertical movement of the wheel axle, and the registration of the stress cell. All these data must be considered simultaneously to arrive at the proper value of a stress at a given point on the tire-soil interface.

In the reduction of the test data for this study, the shape of the deflected tire cross-section was determined at 5-deg intervals of rotation. The positions of the stress cells were then located on each cross-section. From these plots the circumferential position for each cell was determined. Each of the cell registrations, which represent the stress variation over the length of the tire contact area at a particular distance from the center line of the tire, was then properly oriented relative to the deflected tire. These registrations were readily converted to stresses by means of the cell calibrations, and as such, when projected on a horizontal plane, represented longitudinal sections of the total

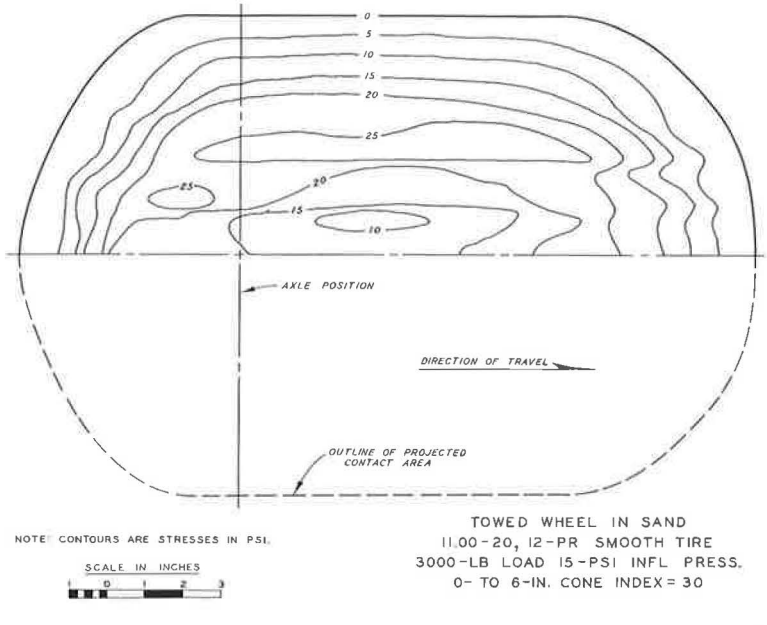

Figure 7. Distribution of normal stresses projected on horizontal plane.

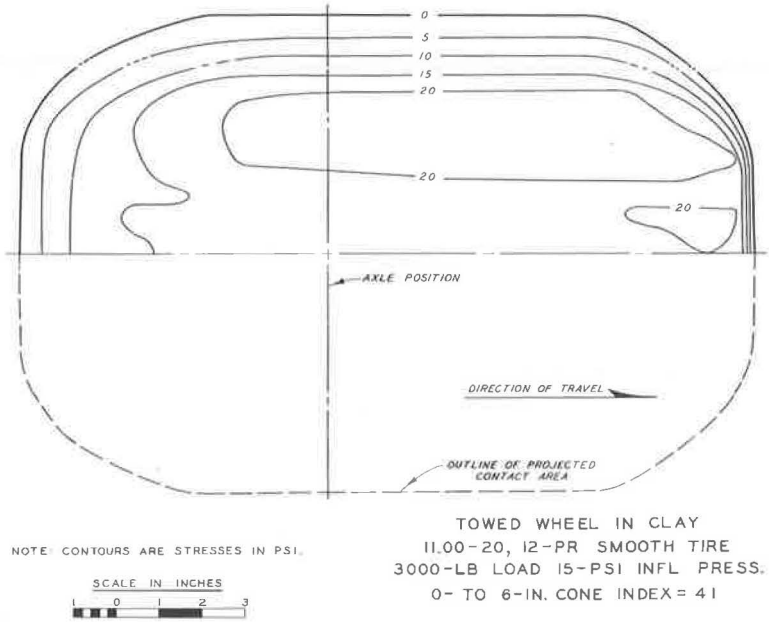

Figure 8. Distribution of normal stresses projected on horizontal plane.

stress pattern. From the longitudinal sections and the recorded distance that each cell was offset from the center line of the tire, a plan of the dynamic tire-contact patch was drawn and on it a map of equal stress lines was constructed.

Stress-Distribution Maps

Figures 7 and 8 show typical stress maps developed from the test data. These maps show measured normal stresses on the projection of the three-dimensional curved interface on a horizontal plane. Because the stress cells are considered to register pressures normal to their surface, the components are obtained by locating the cell positions on the appropriate projection and plotting the accompanying stress magnitude at that point. The maps in Figures 7 and 8 show the distribution of interface stresses beneath the 11.00-20 tire with a 3,000-lb wheel load at an inflation pressure of 15 psi in soft sand and in clay, respectively.

The average cone index in the top 6 in. was greater for the clay. The clay had a cohesive strength of 3.3 psi and its friction angle was 0. The sand at a cone index of 30 had a friction angle of approximately 31 deg and was essentially cohesionless. An effort was made to select a pair of tests in which the maximum "in-soil" deflection was of the same order of magnitude, because this would reflect about equal resistance to displacement and the extent of tire distortion would be about the same in each test. It can be seen that the stresses were most uniformly distributed in the clay, and the high stress zone near the edge of the contact area was not as pronounced as in the sand. The projected contact area was smaller for the clay, indicating that average contact pressure was greater.

Resolution of Resultant Forces

To resolve the normal stresses acting at the tire-soil interface into a single resultant force, the stresses registered by each cell are first plotted normal to a circumference of the deflected tire—the circumference taken at the same offset from the center line of the cross-section of the tire as the cell registering the stresses. Figure 9 is an example of such a plot, showing in this case the circumference of the deflected tire at

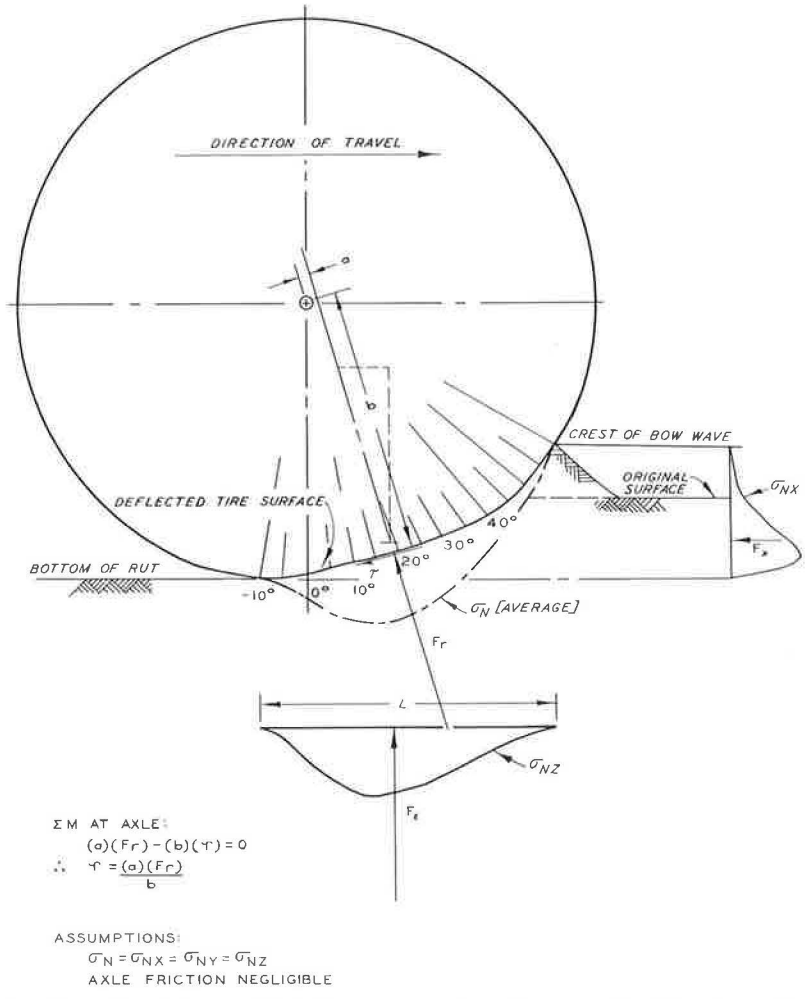

Figure 9. Normal and tangential forces on a towed pneumatic tire in soft soils.

the center line of the cross-section of the tire. The normal stresses registered by a cell at the center line of the tire have been plotted normal to the deflected surface and projected into vertical and horizontal planes. By assuming that the stresses at each point are uniform over some narrow strip whose width is determined by the lateral spacing between the cells, the magnitude and locations of the resultants of the vertical and horizontal components of the normal forces on each strip can be computed. Once this has been done, the magnitudes and the locations of the resultant of the horizontal and vertical components of all the measured normal stresses can be determined and these can be resolved into a single resultant if desired; i. e., the resultant of the normal stresses.

The general validity of the stress cell data and of this approach can be demonstrated to a certain degree for towed tests by comparing the measured horizontal and vertical forces to the computed values. This comparison is good (Table 1).

The computation using the data gathered in this program indicates that the resultant of all the normal stresses at the tire-soil interface appears to intersect the center of the axle for both towed and powered tests. Of 25 towed tests and 7 powered tests analyzed, the resultant normal force always passed within 0. 5 in. of the axle center line. In only six instances was the distance (a, Fig. 9) more than 0. 2 in. In all cases where

TABLE 1

COMPARISON OF COMPUTED AND MEASURED FORCES

Average 0- to 6-In. Cone Index	Inflation Pressure (psi)	Applied Wheel Load (lb)	Measured Towing Force (lb)	Computed	
				Wheel Load (lb)	Towing Force (lb)
(a) Sand					
16	15	3,000	870	2,950	862
15	30	3,000	1,028	2,961	1,098
16	60	3,000	1,115	2,914	1,142
24	15	3,000	760	3,230	703
30	15	3,000	609	3,104	563
27	60	3,000	1,000	3,032	1,124
57	15	3,000	166	3,130	187
54	60	3,000	943	3,147	1,083
(b) Clay					
41	15	3,000	405	3,028	412
47	30	3,000	712	3,260	765
45	60	3,000	755	3,323	797
28	15	3,000	1,020	2,990	1,220
29	30	3,000	1,135	2,986	1,365
28	60	3,000	1,180	2,980	1,208

the resultant, F_r did not intersect the center of the axle, it passed forward of the center line of the axle.

If the resultant of the normal force passes through the axle, it creates no moment about the axle. This suggests that the resultant of the tangential stress must be zero, or very nearly so, for a towed test. However, negative slip is known to occur in a towed test (i.e., the wheel skids slightly), and slip must be accompanied by some tangential forces. Therefore, a tangential force acting in the direction opposite to the slip-induced force must be set up at the interface. Apparently this counterbalancing force is produced by the formation of a bow wave of soil in front of the wheel. By the same token it appears that in powered-wheel tests the resultant of the tangential stresses is directly related to the torque input and the deflected radius of the tire.

Stress Patterns

To give some indication of the distribution of stresses at the tire-soil interface without showing complete stress maps, the stresses measured by a cell at the center line of the tire's cross-section and a cell at an offset of 3.75 in. are shown in Figures 10 through 15. The drawings of the deflected tire and the location of the soil surfaces shown in these figures refer only to the center line of the tire.

RESULTS OF TESTS IN SAND

Towed Tire

Analysis of the results of the towed tire tests in sand indicated that the general shape of the stress patterns tends to be different for each of the three different tire deflections studied. The drawings in Figure 10 are intended to illustrate the three different general types of stress-distribution patterns that could be distinguished in these tests.

The stress patterns shown in plot a of Figure 10 are typical of those from tests in which the in-soil tire deflection was small, usually less than 10 percent. These patterns are identified by the single-peaked curves, both at the center line and at the offset. Tests in which the in-soil tire deflection was greater than about 20 percent usually produced curves of the type shown in plot c of Figure 10. For these tests, the center-line cell always exhibited two maxima in the stress wave, and the cell at the 3.75-in. offset

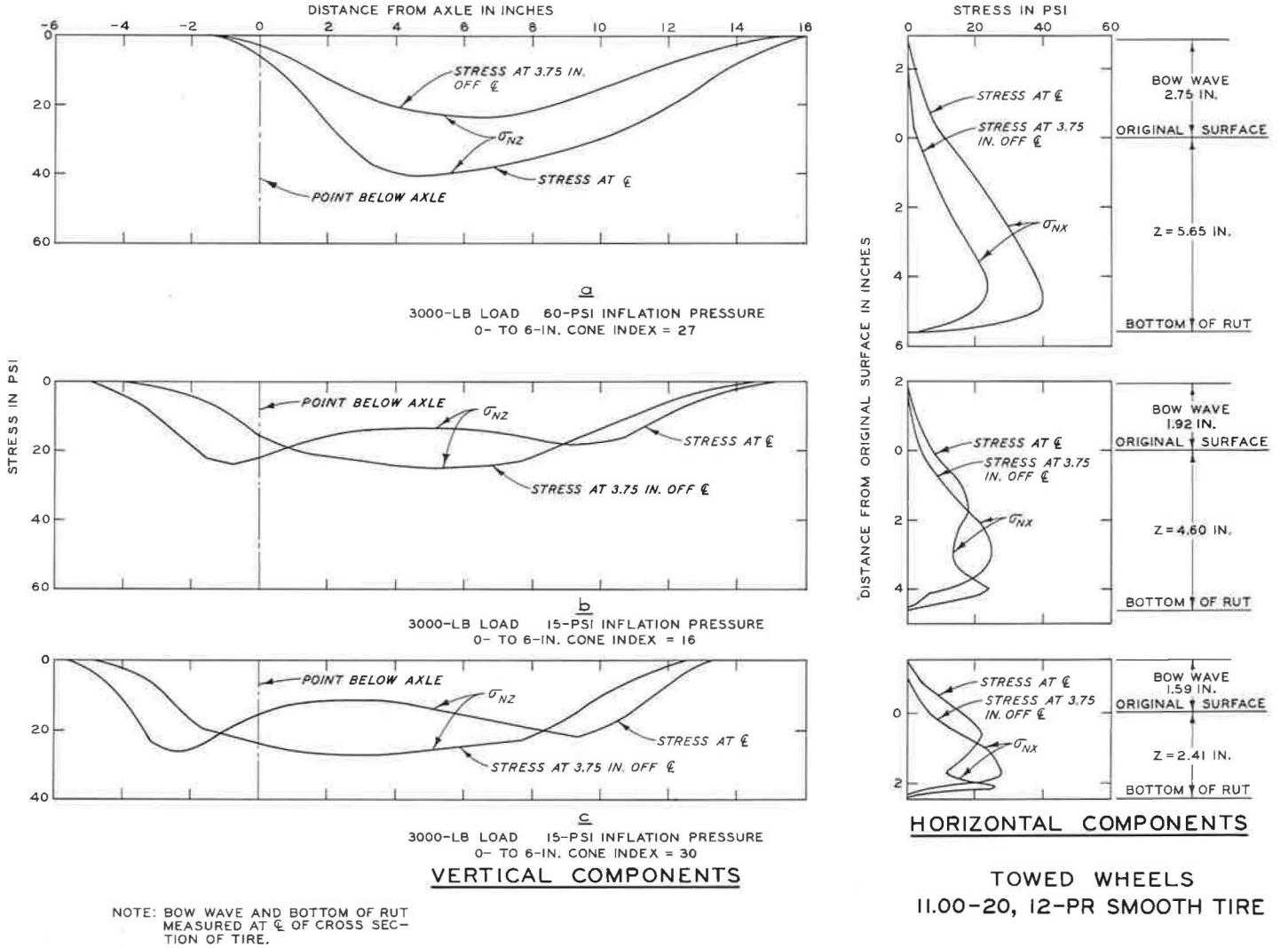

Figure 10. Normal stresses at tire surface in sand.

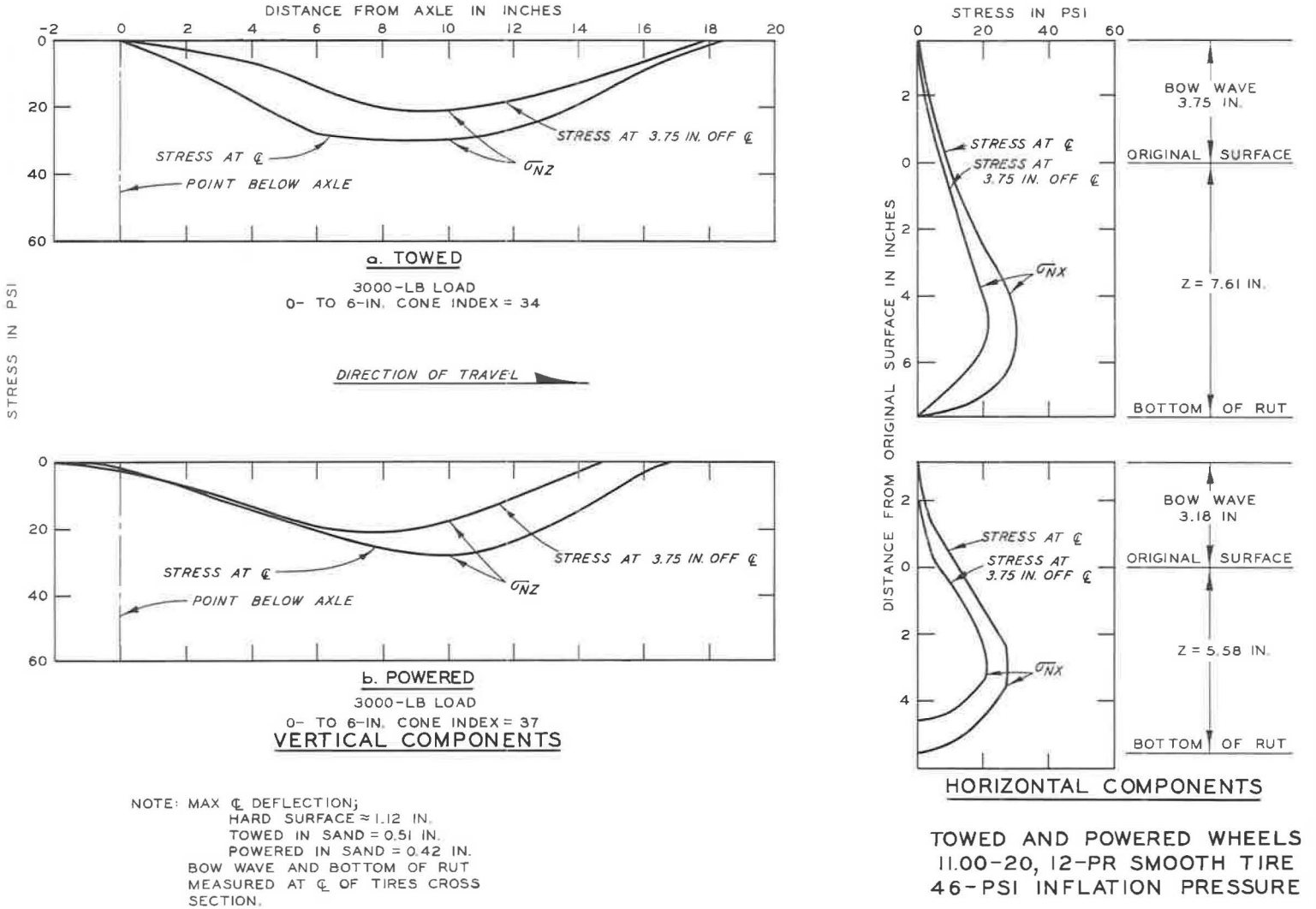

NOTE: MAX ℄ DEFLECTION;
HARD SURFACE ≈ 1.12 IN.
TOWED IN SAND = 0.51 IN.
POWERED IN SAND = 0.42 IN.
BOW WAVE AND BOTTOM OF RUT MEASURED AT ℄ OF TIRES CROSS SECTION.

Figure 11. Normal stresses at tire surface in sand.

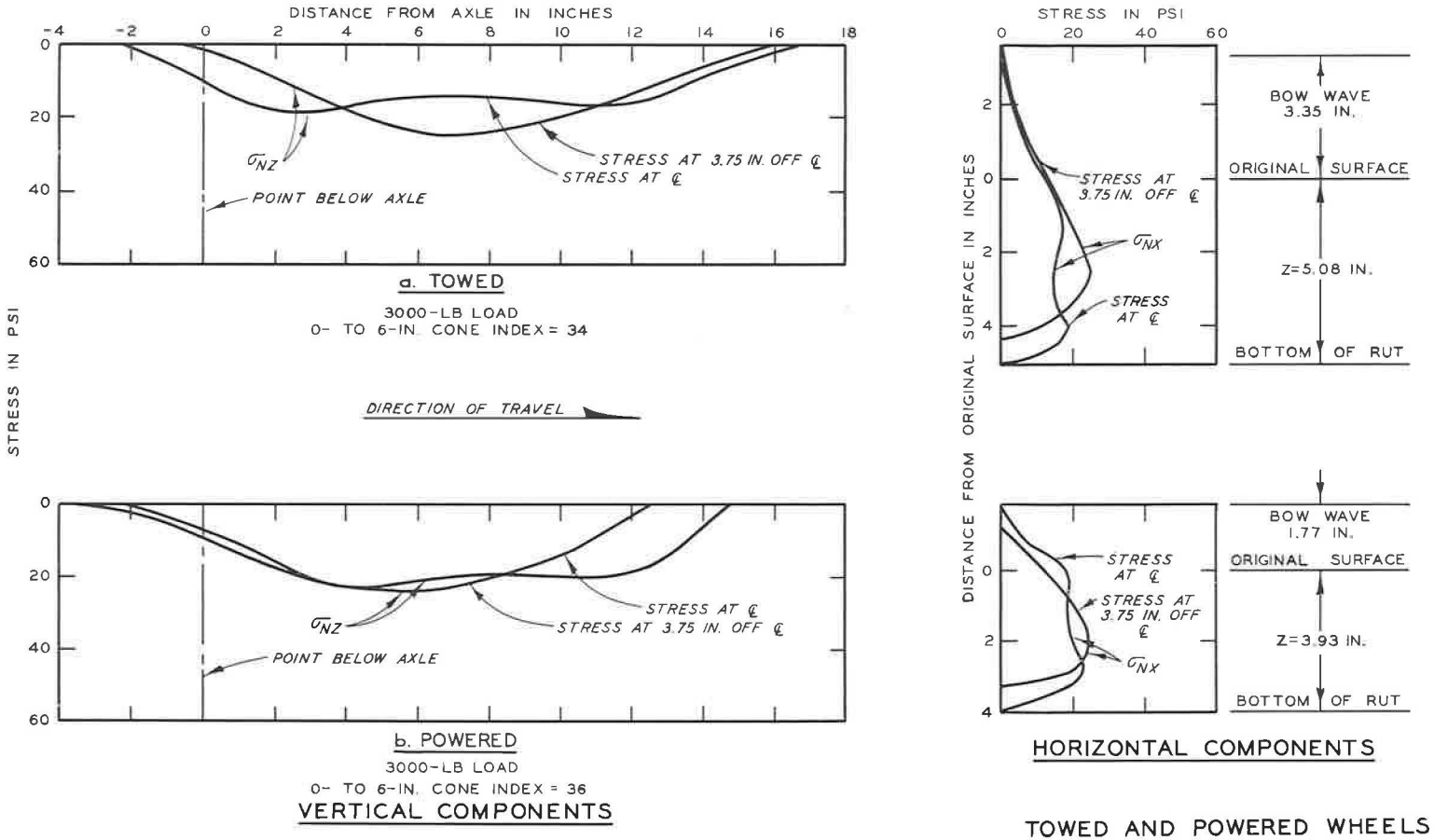

NOTE: MAX ℄ DEFLECTION:
HARD SURFACE ≈ 2.1 IN.
TOWED IN SAND = 1.48 IN.
POWERED IN SAND = 1.42 IN.
BOW WAVE AND BOTTOM OF RUT MEASURED AT ℄ OF TIRES CROSS SECTION

TOWED AND POWERED WHEELS
11.00-20, 12-PR SMOOTH TIRE
19-PSI INFLATION PRESSURE

Figure 12. Normal stresses at tire surface in sand.

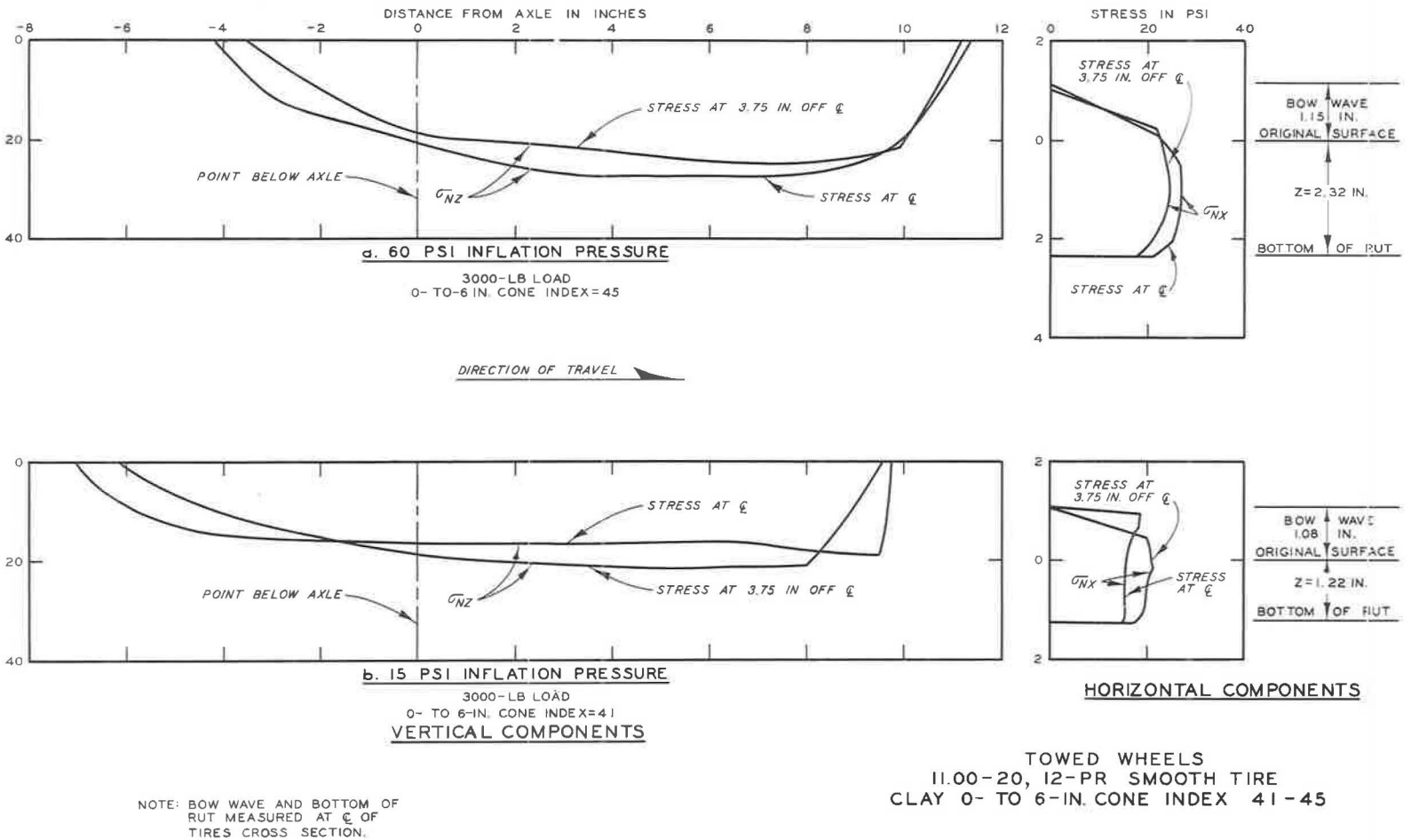

Figure 13. Normal stresses at tire surface in clay.

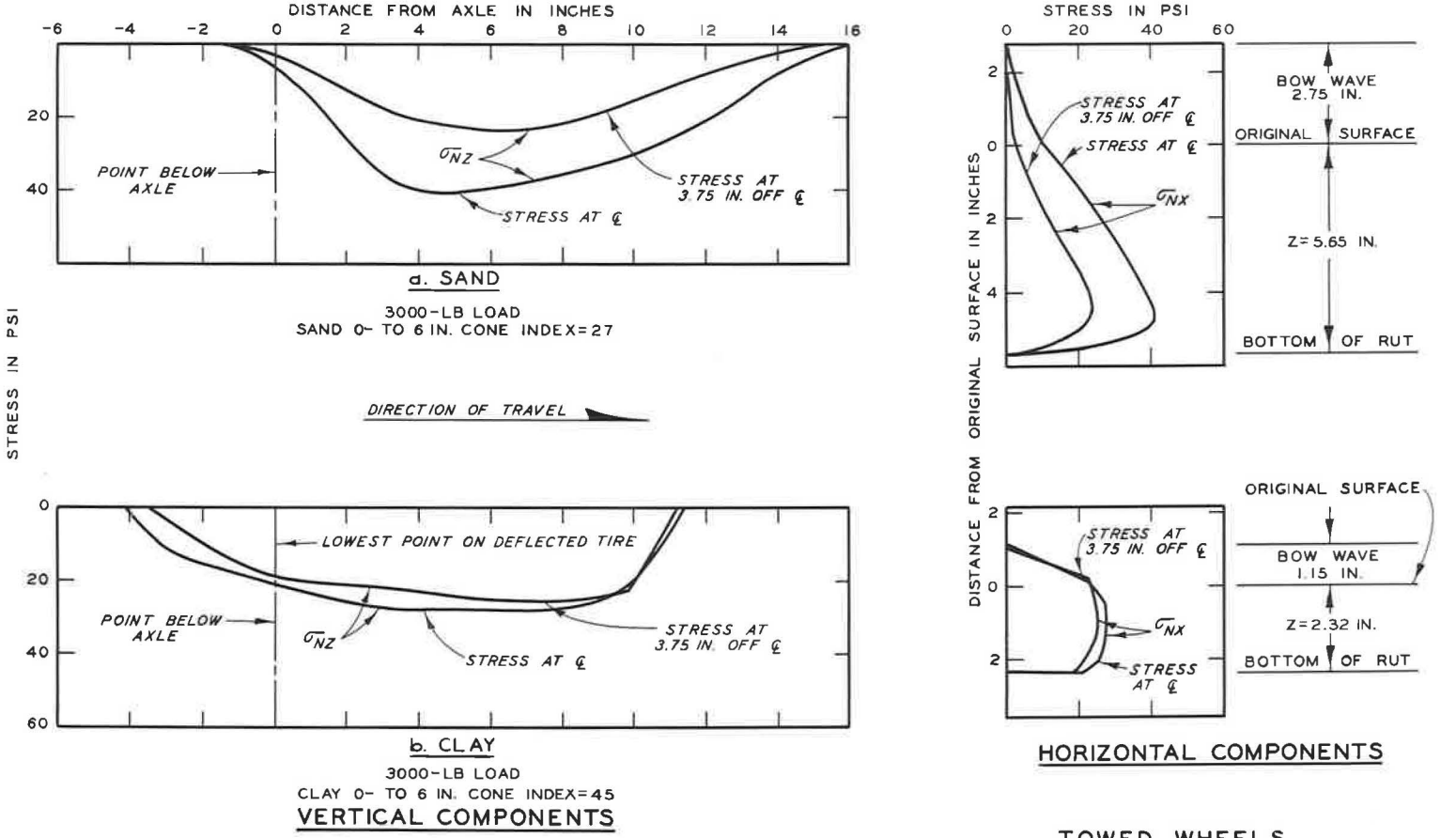

NOTE: MAX ℄ DEFLECTION;
IN SAND = 0.45 IN.
IN CLAY = 0.32 IN.
BOW WAVE AND BOTTOM OF RUT MEASURED AT ℄ OF TIRES CROSS SECTION.

TOWED WHEELS
11.00-20, 12-PR SMOOTH TIRE
60-PSI INFLATION PRESSURE

Figure 14. Normal stresses at tire surface in sand and clay.

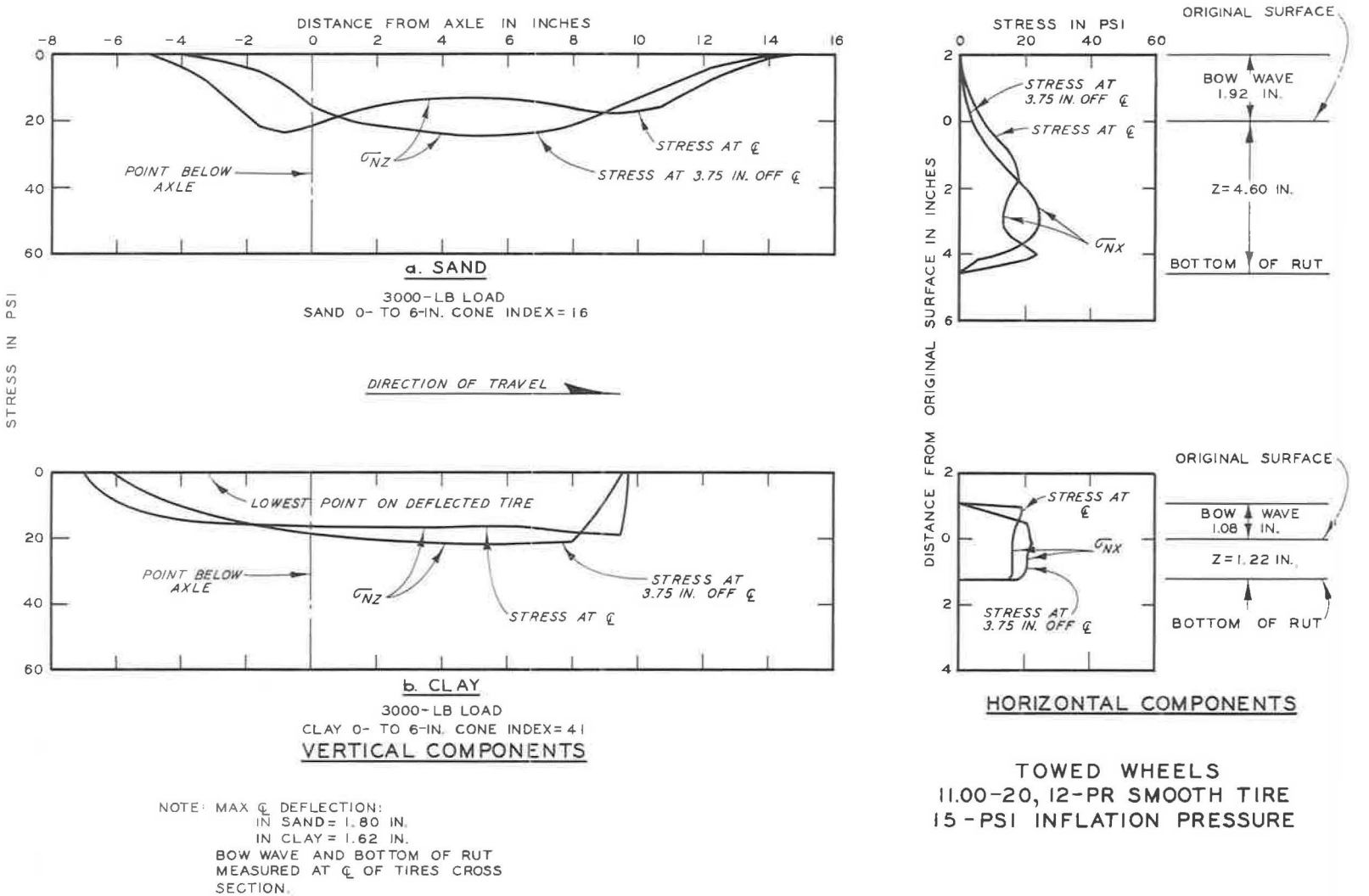

NOTE: MAX ℄ DEFLECTION:
IN SAND = 1.80 IN.
IN CLAY = 1.62 IN.
BOW WAVE AND BOTTOM OF RUT MEASURED AT ℄ OF TIRES CROSS SECTION.

Figure 15. Normal stresses at tire surface in sand and clay.

produced single-peaked stress waves. The third pattern, shown in plot b of Figure 10, represents the intermediate case between the two just described. The tire deflection usually is between about 10 and 20 percent. The center-line cells and the offset cells tend to show a relatively constant stress for a significant portion of the stress wave; and if the curves produced by all cells are averaged, the average stress at any cross-section is about the same for the major portion of the contact length.

Towed- Versus Powered-Wheel Tests

Figures 11 and 12 display comparisons of results of towed- and powered-wheel tests in sand showing the distribution of stresses on the horizontal and vertical projections of the contact areas. The wheel load was 3,000 lb, and inflation pressures were adjusted to produce hard-surface deflections (percent reduction in carcass section height) of 15 and 25 percent, respectively.

In both figures certain observations can be made. The towed wheel produced a deeper rut than the powered wheel under similar conditions of load, deflection, and soil. Stresses produced by the bow wave were greater during the powered tests, and although the exact positions are not shown, it is apparent that the centroid of the vertical component of the normal stresses was a greater distance forward of the axle during the powered tests. Although the stress patterns are somewhat different, the general appearance is the same for towed and powered tests at similar conditions and the peak stress values are of the same order of magnitude. In each pair of tests, the maximum center-line deflection is slightly greater for the towed tire.

RESULTS OF TOWED-WHEEL TESTS IN CLAY

Results of tests at a wheel load of 3,000 lb and inflation pressures of 60 and 15 psi are represented in Figure 13. This figure shows the distribution of stresses on the horizontal and vertical projections of the contact area. This particular pair of tests was chosen to illustrate the fact that the stresses remain uniformly distributed for a wide range of deflections. Maximum center-line deflection during the 60-psi test was approximately 3.5 percent, and during the 15-psi test it was approximately 18 percent. The stresses in the center portion of the contact area were higher than those at the offset position during the 60-psi test; the reverse was true during the 15-psi test. Apparently, in this soft, cohesive material a plastic flow condition develops in the soil beneath the tire and thus reduces the possibility that zones of higher stresses may develop at the tire-soil interface as they do during tests in sand.

A COMPARISON OF TOWED TESTS IN SAND AND CLAY

In Figures 14 and 15, the distribution of the components of the normal stresses on the horizontal and vertical projections of the contact areas is shown. The wheel load was 3,000 lb and the inflation pressures were 60 and 15 psi, respectively. To make this comparison, pairs of tests were chosen in which the maximum in-soil deflection was of the same order of magnitude. As previously mentioned, this indicates that the total resistance to displacement and the extent of the tire distortion were about the same in both the sand and the clay tests.

In both figures the following points are obvious: (a) The interface stresses are more evenly distributed during the tests in clay, and the peak stress values recorded are slightly less than those recorded for the tests in sand. (b) At the front of the contact areas, the stresses increase in magnitude at a faster rate during the clay tests, probably because the bow wave in a cohesive material remains an integral part of the soil mass, having about the same cohesive strength as the mass itself, even though it is being deformed, whereas the bow wave in sand is a disturbed material in a very loose condition. (c) The contact lengths and sinkages are larger for the tests conducted in sand when the maximum deflection of the tire in sand and in clay is of the same order of magnitude.

The position of the lowest point on the deflected tire is indicated in Figures 14 and 15. It is seen that rebound of the clay soil produces normal stresses to the rear of the

lowest point on the deflected circumference, which always fell at, or beyond, a point directly beneath the axle. The approximate amount of rebound estimated from the tire-deflection plot for the two tests shown in 0.2 in.

CONCLUSIONS

On the basis of the data presented in this paper, conclusions are as follows:

1. The line of the resultant of the normal stresses at the tire-soil interface passes through the center line of the wheel axle for towed and powered wheels.
2. In sand, the shape of the stress-distribution pattern is related to the magnitude of the maximum in-soil deflection of the moving tire as measured at the center line of the tire cross-section.
3. Interface stresses are more evenly distributed when the tire is operating in a soft clay soil than when it is operating in sand; i.e., zone of higher stresses is not as pronounced and the peak stress values reached are slightly less than those recorded during a sand test.

REFERENCES

1. D. R. Freitag and A. J. Green. Distribution of Stresses on an Unyielding Surface Beneath Pneumatic Tires. Highway Research Board Bull. 342, pp. 14-23, 1962.
2. U. S. Army Engineer Waterways Experiment Station, CE, Trafficability of Soils, A Summary of Trafficability Studies Through 1955. Tech. Memo. 3240, 14th Suppl., Vicksburg, Miss., Dec. 1956.